

Developmental Cell, Volume 57

Supplemental information

DNGR-1-tracing marks an ependymal cell subset

with damage-responsive neural stem cell potential

Bruno Frederico, Isaura Martins, Diana Chapela, Francesca Gasparrini, Probir Chakravarty, Tobias Ackels, Cécile Piot, Bruna Almeida, Joana Carvalho, Alessandro Ciccarelli, Christopher J. Peddie, Neil Rogers, James Briscoe, François Guillemot, Andreas T. Schaefer, Leonor Saúde, and Caetano Reis e Sousa

Figure S1

Clec9a^{+/-} Rosa^{+tdTomato}

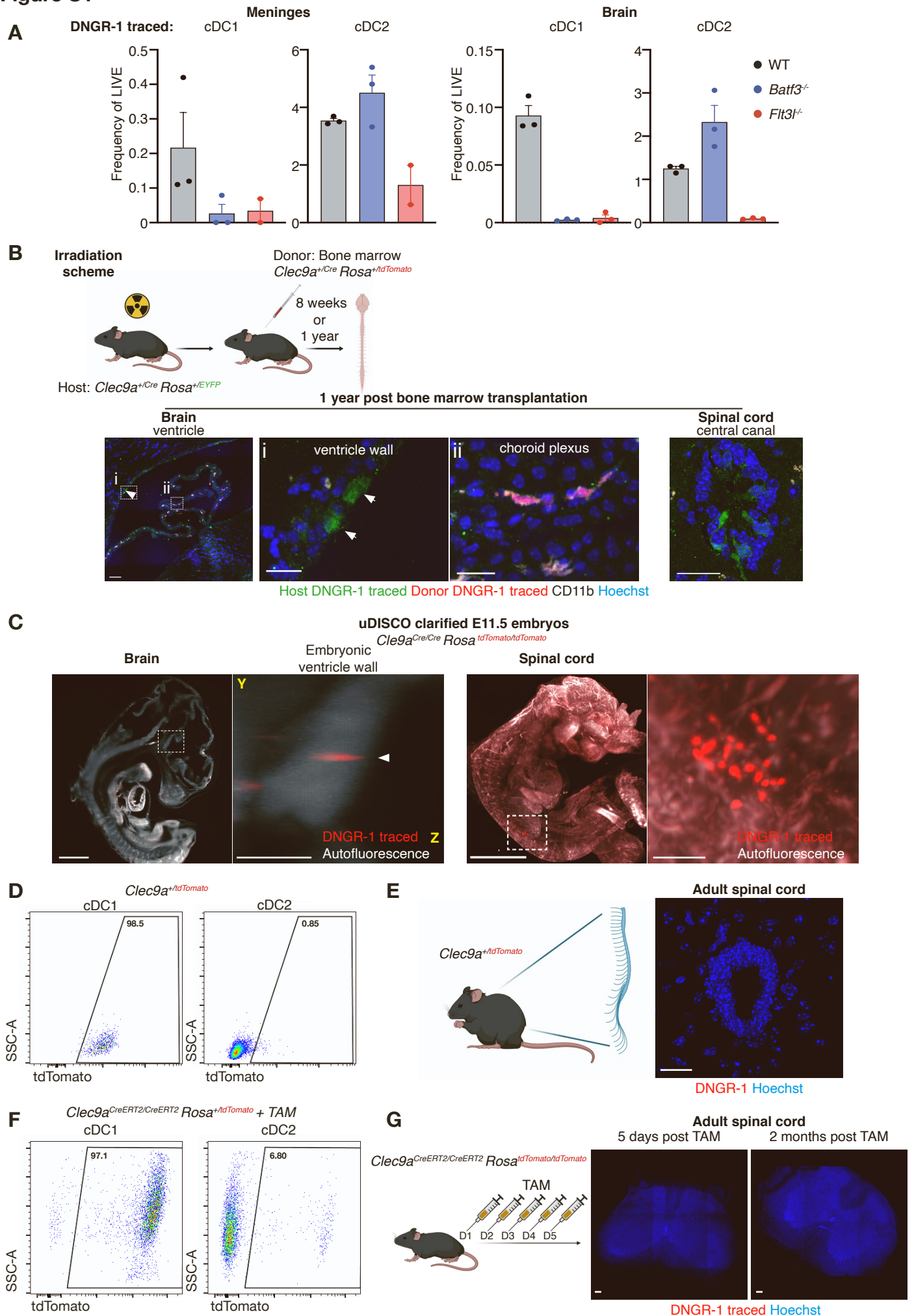


Figure S2

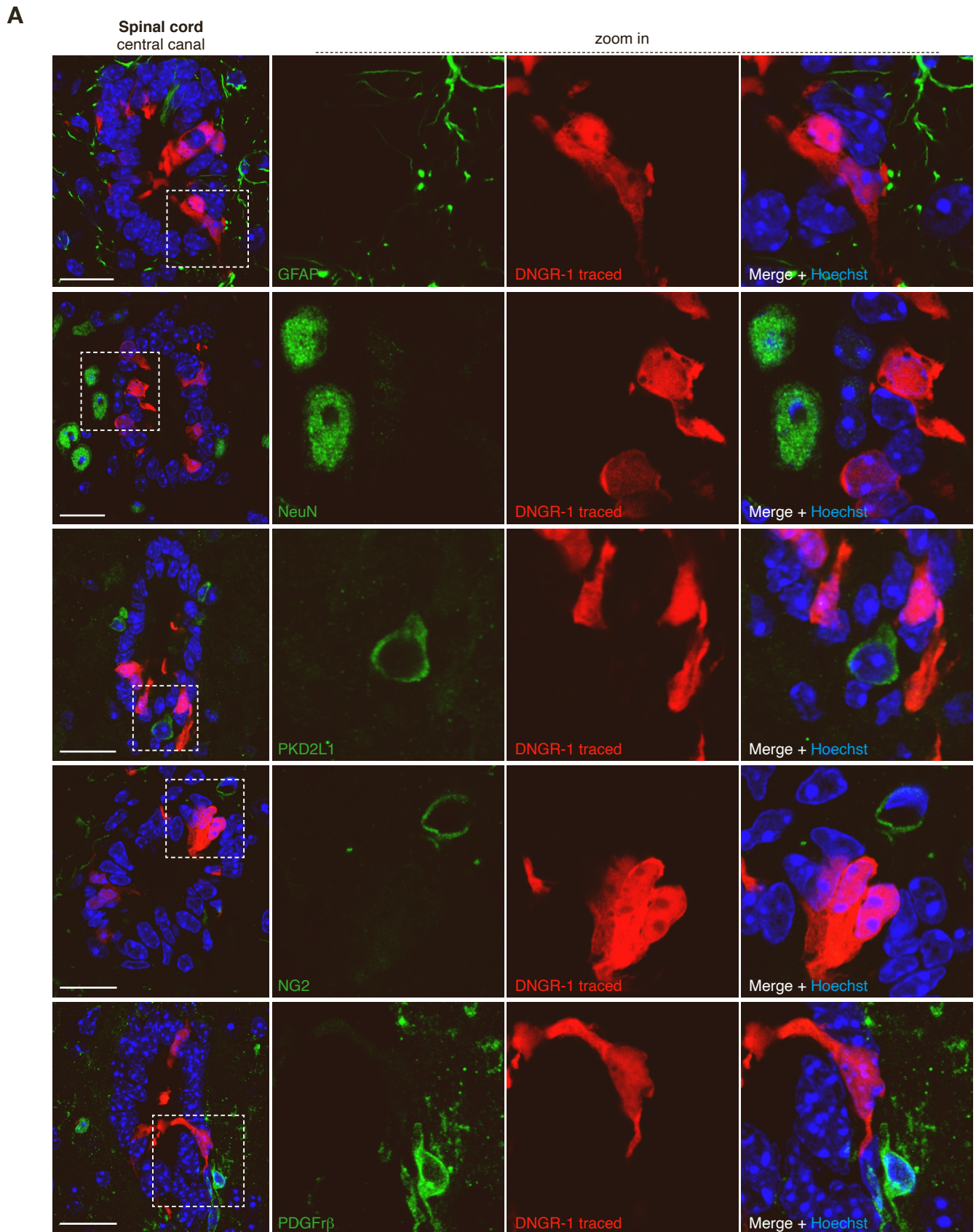
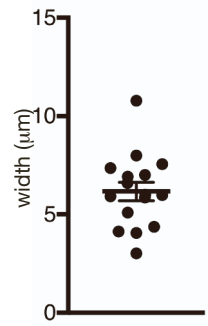
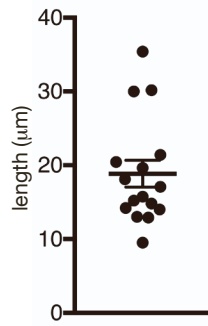
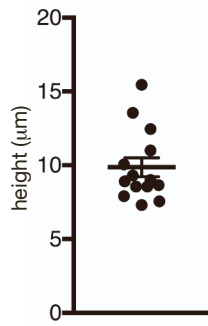
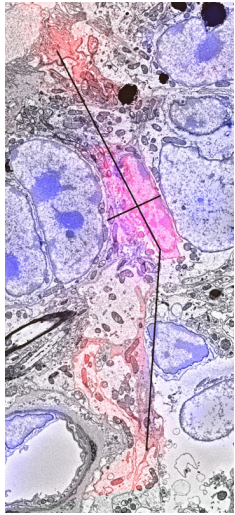
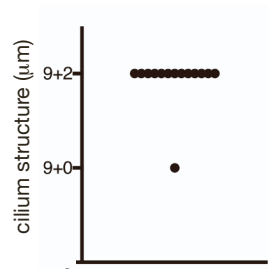
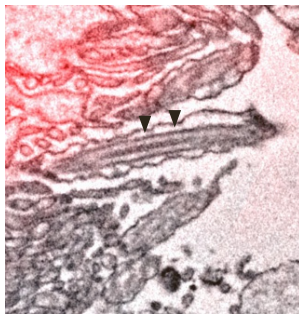


Figure S3

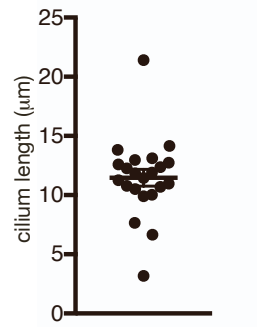
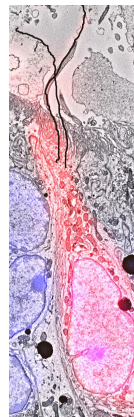
A



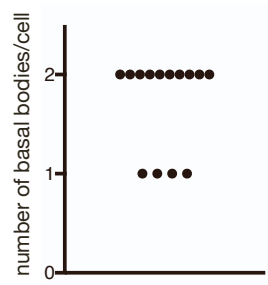
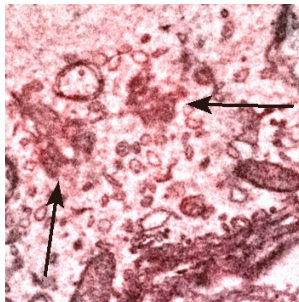
B



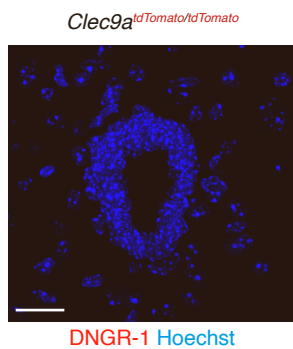
C



D

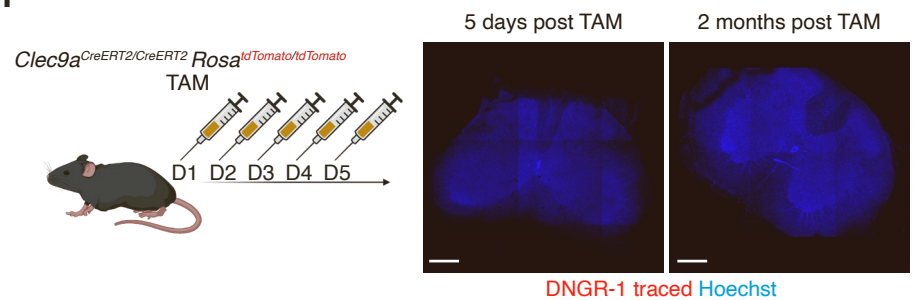


E



DNGR-1 Hoechst

F



DNGR-1 traced Hoechst

Figure S4

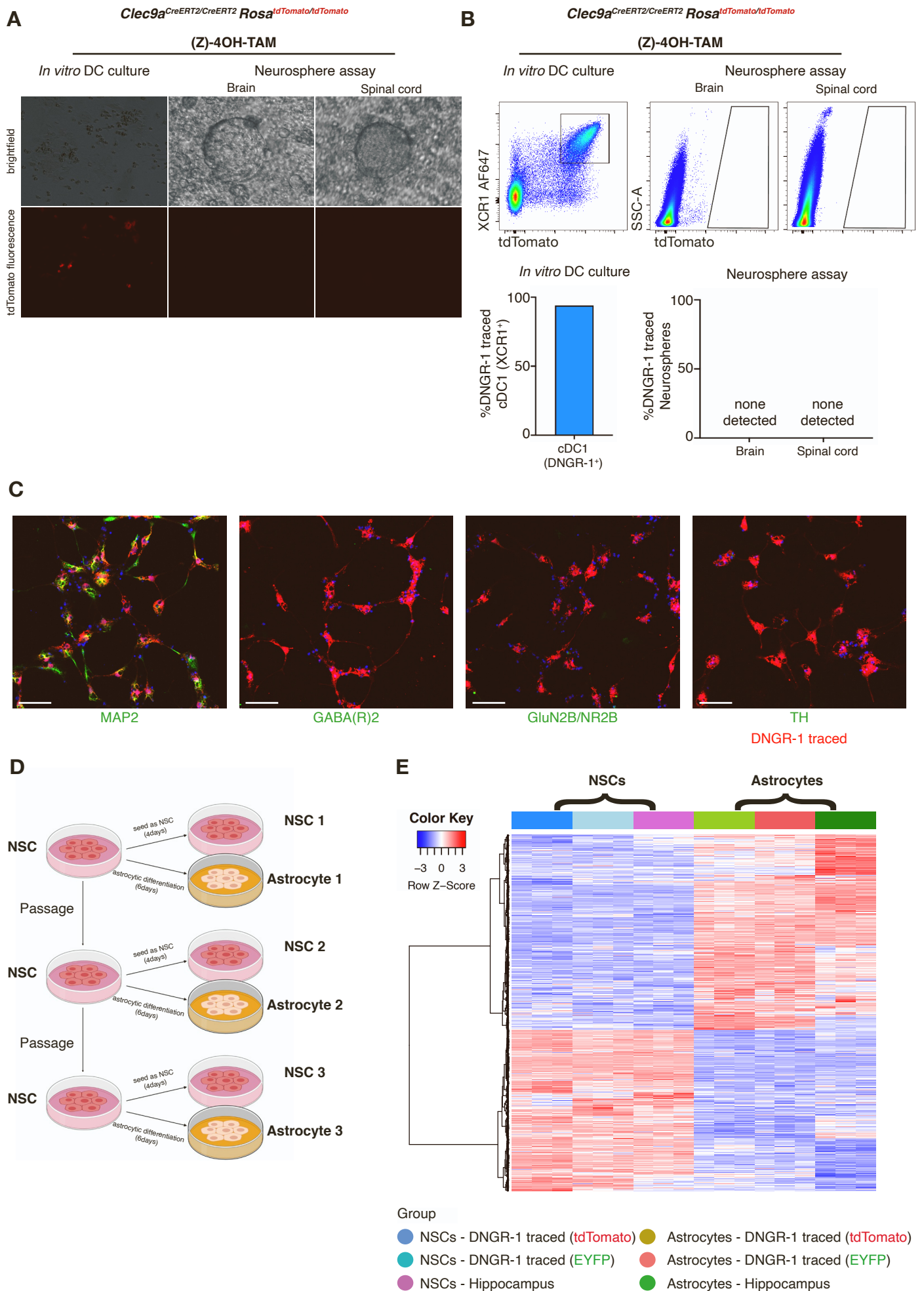


Figure S5

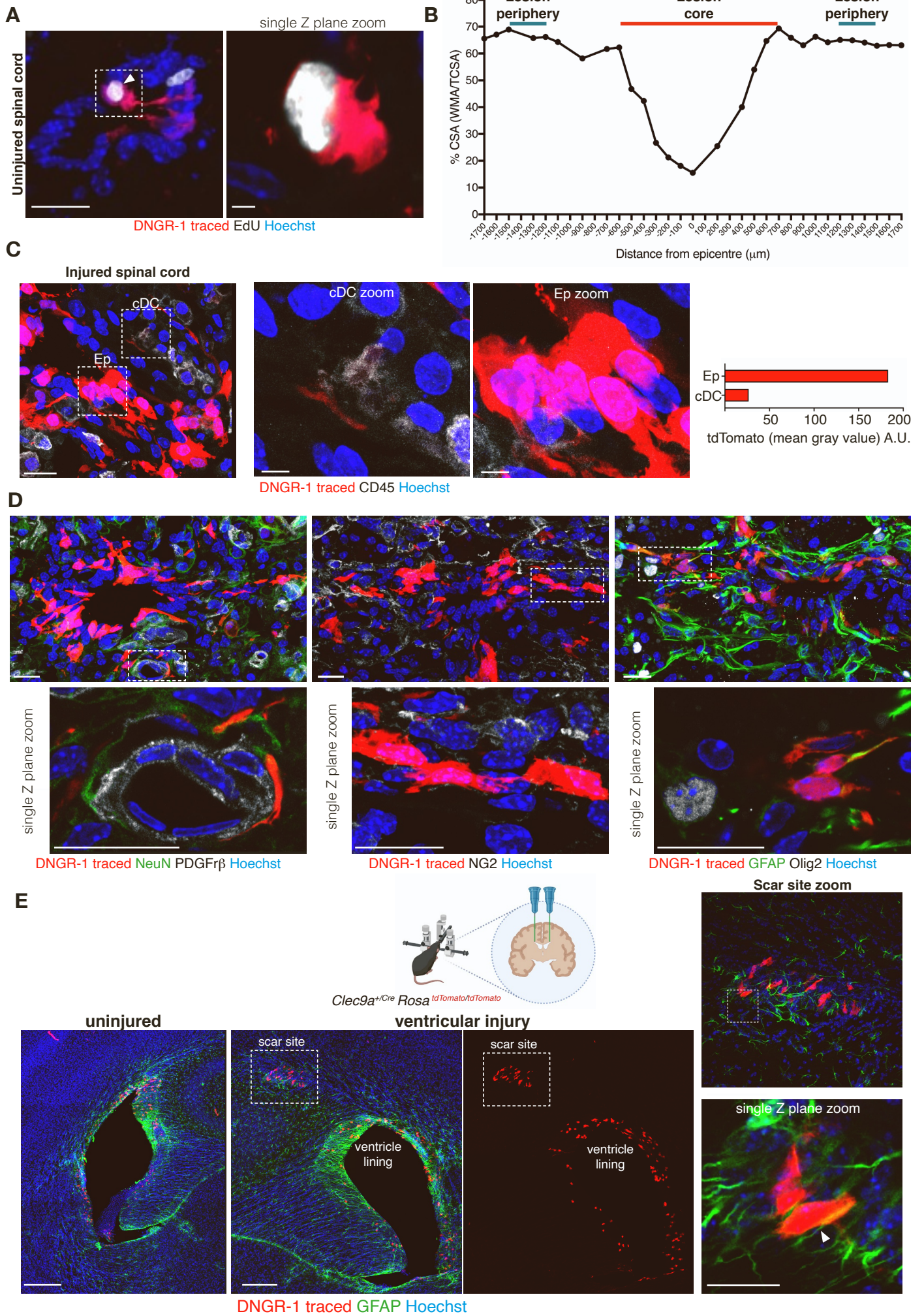


Figure S6

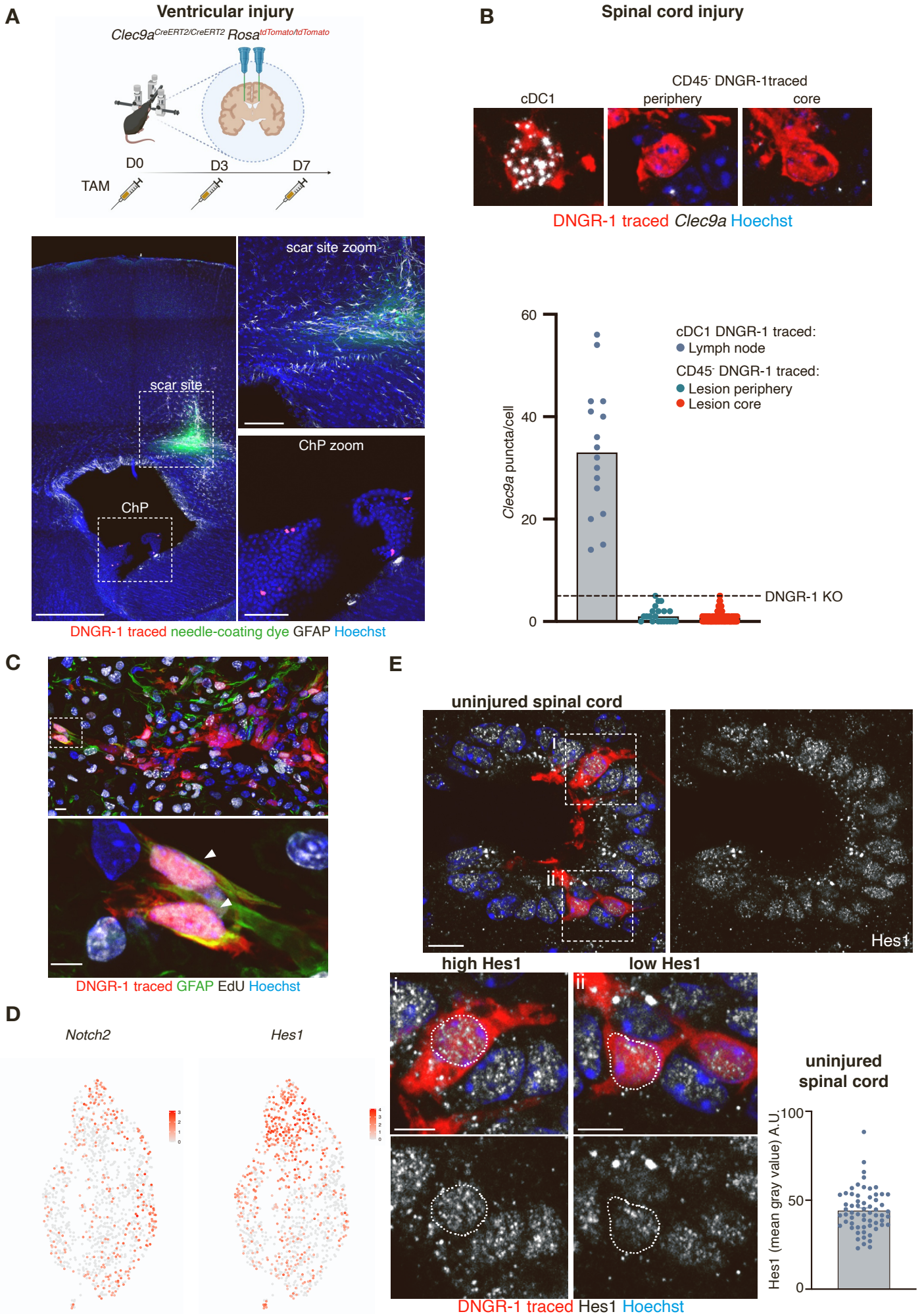
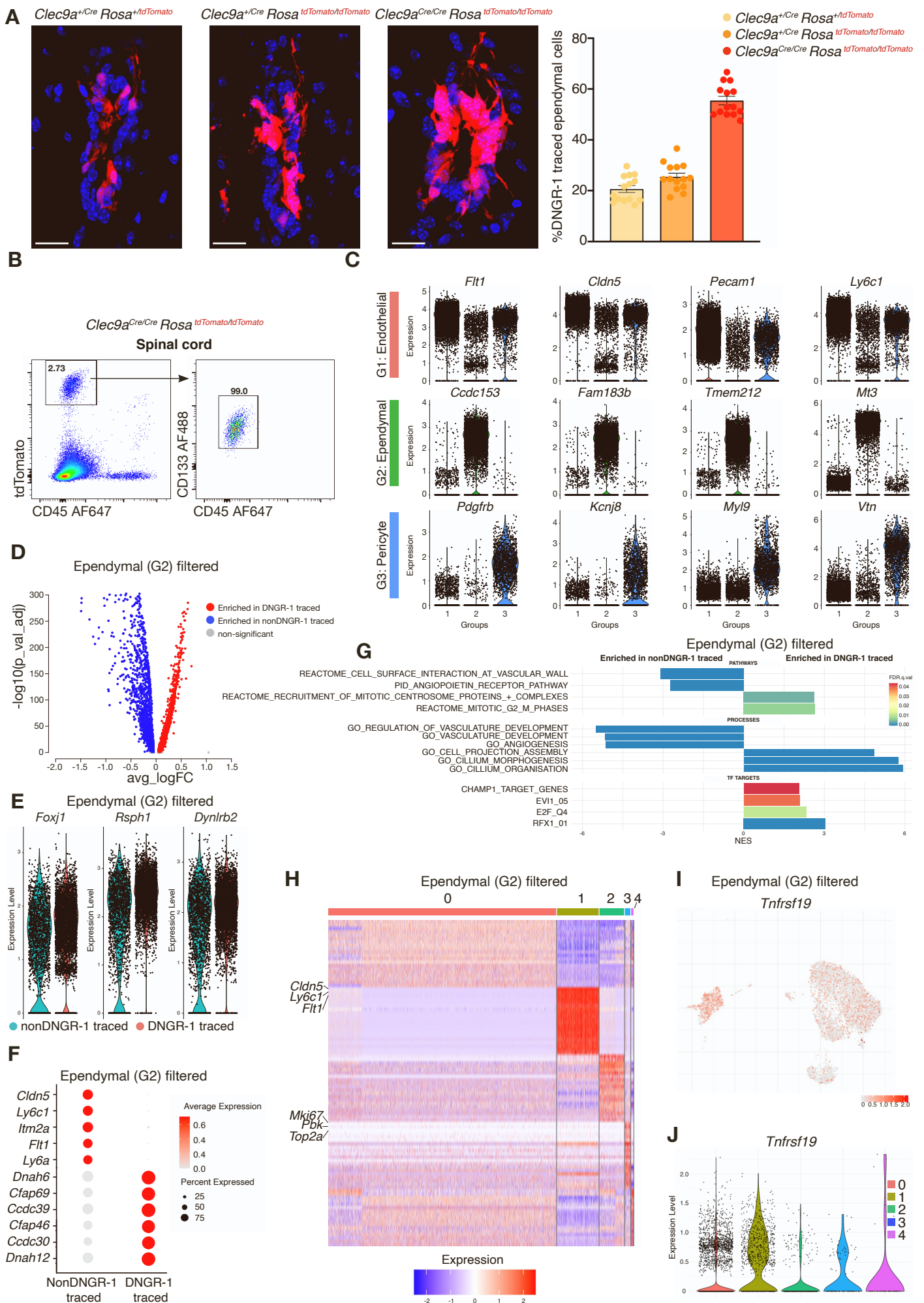


Figure S7



Supplemental figure legends

Figure S1 | CD45⁺ DNGR-1 traced are unrelated to cDCs. Related to Figure 2.

A. Flow cytometry quantification of DNGR-1 traced cDC1 or cDC2 in the meninges or choroid plexus of *Clec9a^{Cre}Rosa^{LSLtdTomato}* mice lacking *Batf3* or *Flt3l* (n=3 animals/group). Leucocytes were enriched in brain samples using a percoll gradient. Each dot represents one animal.

B. Irradiation scheme and immunofluorescence of CNS from irradiated *Clec9a^{Cre}Rosa^{LSLEYFP}* bone-marrow chimeric animals, 1 year post transplantation with *Clec9a^{Cre}Rosa^{LSLtdTomato}* bone marrow (n=3). Zoomed in areas show **i**) host-derived DNGR-1 traced ependymal cells (EYFP⁺, green) lining the ventricle wall; and **ii**) a CD11b⁺ (white) donor-derived haematopoietic DNGR-1 traced cells (red) in the choroid plexus. Right, all DNGR-1 traced cells in the spinal cord central canal were of host origin (EYFP, green).

C. Optically clarified and light-sheet imaged E11.5 *Clec9a^{Cre}Rosa^{LSLtdTomato}* embryos showing DNGR-1 traced cells (red) embedded in the embryonic brain ventricle wall or spinal cord. Right, zoomed view of areas indicated with dashed outlines. Ventricle wall zoom is an orthogonal projection (YZ planes), spinal cord zoom is a maximum intensity projection. 10 embryos were analysed.

D. Flow cytometric analysis of spleens from *Clec9a^{tdTomato}* animals showing percentage of tdTomato-positive cDC1 and cDC2.

E. Immunofluorescence of the spinal cord central canal from an adult *Clec9a^{tdTomato}* animal. No DNGR-1 expressing cells (red) could be observed.

F. Flow cytometric analysis of spleens from *Clec9a^{CreERT2}Rosa^{LSLtdTomato}* animals given tamoxifen (TAM; 5 daily intraperitoneal injections) and examined 5 days after the last injection, showing percentage of DNGR-1 traced (tdTomato⁺) cDC1 and cDC2.

G. Immunofluorescence of the spinal cord central canal from *Clec9a^{CreERT2}Rosa^{LSLtdTomato}* animals 5 days (mice from (F)) or 2 months post tamoxifen administration (5 daily doses; schematic on left). No DNGR-1 traced cells (red) were observed at either time point.

Scale bars, 1mm (**C**, brain), 500µm (**C**, spinal cord), 100µm (**B**, **G**, zooms **C**) and 20µm (**E** and zooms **B**). (**D-E** are representative data of at least 3 animals analysed)

Figure S2 | DNGR-1 lineage-traced cells lining the central canal of the spinal cord are not astrocytes, oligodendrocyte precursors, neurons or pericytes. Related to Figure 3.

A. Immunofluorescence of spinal cord sections from *Clec9a^{cre}Rosa^{LSLtdTomato}* mice with GFAP, NG2, NeuN, PKD2L1, and PDGFrβ (green) and Hoechst (blue). No DNGR-1 traced ependymal cells (red) co-stained with any of the markers. Scale bars 20µm. Images are representative of at least 3 animals.

Figure S3 | Ultrastructural features of DNGR-1 traced spinal cord cells. Related to Figures 3 and 4.

Correlative light-electron microscopy from spinal cord sections from *Clec9a^{Cre}Rosa^{LSLtdTomato}*. DNGR-1 traced cells (red) were interrogated for several ultrastructure features, such as

- A. dimensions;
- B. cilium structure;
- C. cilium length;
- D. number of basal bodies per cell. Images are representative of at least 2 sections from 2 animals.

Figure S4 | Comparison of DNGR-1 traced, hippocampus-derived neural stem cells and their differentiated progeny in culture. Related to Figure 5.

A. Representative wide-field photographs of *in vitro* DC or neurospheres cultures grown from bone marrow or brain/spinal cord of *Clec9a^{CreERT2}Rosa^{LSLtdTomato}* animals, respectively, in the presence of 500nM (Z)-4OH-TAM. (Z)-4OH-TAM was replaced every two/three days. Whilst cDC cultures contained DNGR-1 traced cells, no DNGR-1 traced neurospheres were observed (>500 neurospheres/ organ analysed)).

B. Flow cytometric quantification of (A). Data are representative of two independent experiments.

C. Immunofluorescence of DNGR-1 traced neuronal differentiation cultures stained with antibodies against pan (MAP2) or mature neuronal markers TH (tyrosine hydroxylase), NR2B (NMDA receptor 2B) or GABA(B)R2 (GABA-B-receptor 2), all green; blue, DAPI; scale bar, 20 μ m. Data are representative of two independent experiments.

D. Schematic representation of sample preparation for bulk RNA sequencing.

E. Heatmap of differential expressed genes between NSC and astrocyte cell fates.

Figure S5 | Differentiation of DNGR-1 traced ependymal cells after spinal cord injury is restricted to the astrocytic lineage. Related to Figure 7.

A. Immunofluorescence of central canal from uninjured *Clec9a^{cre}Rosa^{LSLtdTomato}* mice after EdU pulse. Arrowhead indicates a DNGR-1 lineage traced ependymal cell (red) which has incorporated EdU (white). Right, single optical Z plane of dashed boxed area showing nuclear localization of EdU signal.

B. White matter sparing at 7 days post spinal cord injury across the injury length, as described in the methods section. Each point equals one measurement. Values plotted derive from one

representative animal. CSA (Cross section area), WMA (white matter area), TCOSA (total cross section area).

C. Immunofluorescence of injured spinal cord sections from *Clec9a^{Cre}Rosa^{LSLtdTomato}* mice with CD45 showing low tdTomato brightness in DNGR-1 traced cDCs and high tdTomato brightness in DNGR-1 traced ependymal cells. Scale bar, 20 μ m, zooms, 5 μ m.

D. Immunofluorescence of injured spinal cord sections from *Clec9a^{Cre}Rosa^{LSLtdTomato}* mice with NeuN or GFAP (both green), PDGFr β , NG2 or Olig2 (all white) and Hoechst (blue). DNGR-1 traced ependymal cells (red) co-stained only with GFAP. Images are representative of at least 3 animals. Right, single optical Z planes of dashed boxed areas.

Scale bars 20 μ m.

E. Schematic representation of ventricular injury of *Clec9a^{Cre}Rosa^{LSLtdTomato}* mice and vibratome sections of uninjured or 28 days post-injury brains stained for GFAP (green) and with Hoechst (blue). Uninjured brains show showing DNGR-1 traced cells (red) residing exclusively in the ependymal layer and not expressing GFAP. Post-injury, DNGR-1-traced cells (red) can be seen dislodged from the ependymal layer and accumulating around the scar site where some cells express GFAP. Zooms show areas defined by dashed outlines. Arrowhead in lower panel zoom indicates a GFAP⁺ DNGR-1-traced cell in the scar site. Images are representative of three injured animals. Scale bars, 300 μ m (uninjured brain) 200 μ m (injured brain), 100 μ m (upper panel zoom) and 20 μ m (lower panel zoom).

Figure S6 | DNGR-1 traced ependymal cells do not re-express DNGR-1 after injury. Related to Figure 6.

A. Schematic representation of ventricular injury model applied to *Clec9a^{CreERT2}Rosa^{LSLtdTomato}* animals. Tamoxifen was injected intraperitoneally 1-2hrs prior to injury and at days 3 and 7 post injury. Vibratome section of a brain 28 days post-injury showing an astrocytic scar at the place where injury was inflicted (marked in this experiment by a needle-coating dye signal, green). No DNGR-1 traced cells were observed in the ventricular wall or at the scar site. DNGR-1 traced cells were only observed in the choroid plexus, consistent with their dendritic cell nature. Zooms showing areas defined by dashed outlines. Arrowhead indicates a GFAP⁺ DNGR-1-traced cell in the scar site. Images are representative of three injured animals. Scale bars, 500 μ m (overview) 100 μ m (zooms).

B. Detection of *Clec9a* transcripts by single molecule fluorescence *in situ* smFISH in lymph nodes or injured spinal cords from *Clec9a^{+cre}Rosa^{LSLtdTomato}* animals. DNGR-1⁺ traced cDC1s (red) show abundant *Clec9a* expression (white puncta) as expected. Below, quantification of *Clec9a* puncta per cell indicated. Horizontal dotted line indicates background level as

determined by the maximum number of puncta observed in DNDR-1 deficient animals (*Clec9a^{cre/cre}Rosa^{LSLtdTomato}*) (n=5).

C. Immunofluorescence of DNDR-1 traced astrocytes in an injured spinal cord segment showing staining for EdU (arrowheads).

D. Feature plots showing projection of *Notch2* or *Hes1* expression by DNDR-1 traced ependymal cells on UMAP space. Low expression (grey) and high expression (red).

E. Immunofluorescence of spinal cord central canal from an uninjured *Clec9a^{cre}Rosa^{LSLtdTomato}* mouse and HES1 staining (white). Zooms of dashed boxed areas below show DNDR-1 traced cells (red) displaying **i**) high or **ii**) low HES1 levels. No HES1 negative DNDR-1 traced cells were observed. Right, quantification of Hes1 mean gray value intensity (a.u. arbitrary units). Each dot represents one cell. Quantification across at least 5 animals.

Scale bars, 10 μ m (**C**, **E**), 5 μ m (zooms **C**, **E**).

Figure S7 | Incomplete penetrance does not fully account for partial ependymal cell labelling and comparison between DNDR-1 traced and non-traced ependymal cells. Related to Figure 7.

A. Immunofluorescence images of spinal cord central canal from DNDR-1 tracer mice of different penetrance and quantification of ependymal cell labelling in each genotype. Red, DNDR-1 traced cells. Blue, Hoechst.

B. Flow cytometry enumeration of the proportion of spinal cord non-cDC-DNDR-1 traced cells (CD45⁻, tdtom⁺) stained with anti-CD133.

C. Expression of a selected set of transcripts from the integrated UMAP of CD133⁺ DNDR-1 traced and CD133⁺ non-traced cells (related to Figure 7D).

D. Volcano plot representing the differently expressed genes between DNDR-1 traced and non-traced ependymal cells (G2 filtered). Statistically significant genes enriched in DNDR-1 traced ependymal cells are coloured in red. Statistically significant genes enriched in nonDNDR-1 traced ependymal cells are coloured in blue. Non-statistically significant genes are coloured in grey. Statistical significance threshold = (p<0.05)

E. Violin plots showing expression of canonical ependymal cell genes in DNDR-1 traced and non-traced ependymal cell (G2 filtered populations).

F. Dot plot showing expression of selected top-differentially expressed genes between DNDR-1 traced and non-traced ependymal cells (G2 filtered).

- G.** GSEA analysis showing significant differential enrichment of selected Pathways, Processes and TF targets between DNGR-1 traced and non-traced ependymal cells (G2 filtered).
- H.** Heatmap showing the top 20 differentially expressed genes amongst the clusters belong to group 2 (related to Figure 7G).
- I.** Feature plot showing projection of *Tnfrsf19* transcripts on the UMAP space of ependymal (G2 filtered) population. Low expression (grey) and high expression (red).
- J.** Violin plot showing distribution of *Tnfrsf19 transcripts* across the different ependymal cell clusters (G2 filtered) population.